A Letters Journal Exploring the Frontiers of Physics

April 2009

EPL, **86** (2009) 14006 www.epljournal.org
doi: 10.1209/0295-5075/86/14006

Specific roles of fluid properties in non-Boussinesq thermal convection at the Rayleigh number of 2×10^8

A. Sameen[1], R. Verzicco[2] and K. R. Sreenivasan[3(a)]

[1] *Department of Aerospace Engineering, Indian Institute of Technology Madras - Chennai-600036, India*
[2] *University of Roma "Tor Vergata" - Roma, Italy, EU*
[3] *International Centre for Theoretical Physics - Trieste 34014, Italy, EU*

received 6 September 2008; accepted in final form 11 March 2009
published online 22 April 2009

PACS 47.55.pb – Thermal convection
PACS 47.27.te – Turbulent convective heat transfer
PACS 47.55.P- – Buoyancy-driven flows; convection

Abstract – We demonstrate the specific non-Boussinesq roles played by various fluid properties in thermal convection by allowing each of them to possess, one at a time, a temperature dependence that could be either positive or negative. The negative temperature dependence of the coefficient of thermal expansion hinders effective thermal convection and reduces the Nusselt number, whereas the negative dependence of fluid density enhances the Nusselt number. Viscosity merely smears plume generation and has a marginal effect on heat transport, whether it increases or decreases with temperature. At the moderate Rayleigh number examined here, the specific heat capacity shows no appreciable effect. On the other hand, the conductivity of the fluid near the hot surface controls the heat transport from the hot plate to the fluid, which suggests that a less conducting fluid near the bottom surface will reduce the Nusselt number and the bulk temperature.

Introduction. – The flow generated by the buoyancy force in a fluid column between two horizontal plates maintained at different temperatures has been a topic of intense research [1,2]. An important control parameter for the problem is the Rayleigh number $Ra \equiv \alpha \Delta T g H^3/\nu\kappa$, where α is the isobaric thermal expansion coefficient of the fluid; ΔT, the temperature difference between the top and bottom plates separated by a vertical height H; g, the acceleration due to gravity; ν, the kinematic viscosity; and κ, the thermal diffusivity of the fluid. It is also known that the flow characteristics depend on the geometry and the Prandtl number $Pr = \nu/\kappa$.

If the temperature difference ΔT is small so that the resulting density differences in the flow are small as well, it is traditional to account for the effects of density variations only through the gravitational body force and to assume, in so far as all other effects are concerned, that constant density is a good approximation. This is the Boussinesq approximation. If this approximation is invalid, one has to account for the temperature variations of all fluid properties. A comprehensive account of the non-Boussinesq effects near the onset of the primary instability of the flow can be found in [3,4], but our understanding of their precise role in the turbulent regime, which began with ref. [5] and explored more recently [6–13], is still inadequate.

Reference [9] attempts to understand the effect of the non-Boussinesq effects in water and glycerol experimentally. The temperature dependence of kinematic viscosity and thermal diffusion coefficient were found to have a dominant influence on center temperature. However, they did not isolate the role of individual physical properties in determining the heat transport or center temperature. Reference [10] uses ethane gas and notes that the center temperature decreases for gases and the Nusselt number increases for large non-Boussinesq values at Rayleigh numbers that are higher than that reported in this paper. For gases, it is noted that the center temperature is less than the algebraic mean of the top and bottom temperatures, as obtained in [10,11,13], but a physical reason is not elucidated. Two-dimensional DNS in refs. [11,12] of Rayleigh-Bénard convection with properties of glycerol and ethane, respectively, tries to dwell into the non-Boussinesq effects on the center temperature at low Rayleigh numbers, and again falls short of giving a physical picture of the role of fluid properties.

(a) E-mail: krs@ictp.it

The experimental part in ref. [11] chooses a temperature difference on either side of critical point thus enabling the experimentalists to get a positive or negative variation of fluid properties with temperature. Ahlers *et al.* note that for ethane, the variations of expansivity and specific heat capacity were larger than those of other properties, and attribute the change in the center temperature from the Boussinesq value to these two properties. For gas-like variations (negative α and $C_{\rm p}$) they find a decrease in the center temperature and *vice versa* for liquid-like variations, and suggest a combined effect of α and $C_{\rm p}$, with nonlinear effects from other property variations. It will be shown that the present computation matches well with these results qualitatively, even though the non-Boussinesq effects found in the experiments were for higher Rayleigh number. The Nusselt number effects are, however, found to increase irrespective of liquid-like or gas-like variation in [11], unlike the results shown here. We stress that, results shown here isolate the role of each property and hence a direct comparison with [11] is not completely possible, especially for the lower Rayleigh number considered here. In addition to the response of bulk temperature and Nu to various properties, we also provide a physical picture of a likely mechanism in thermal convection.

In this paper we attempt to understand these effects by varying each fluid property separately while keeping all the others fixed. We do this by resorting to direct numerical simulations of the full equations of motion, including non-Boussinesq effects. Five fluid properties affect Rayleigh-Bénard convection: 1) dynamic viscosity, μ; 2) density, ρ; 3) coefficient of thermal expansion, or the expansivity, α; 4) thermal conductivity, λ; and 5) specific heat at constant pressure, $C_{\rm p}$. These properties may increase or decrease with temperature depending on whether the fluid is a liquid or a gas, or is in an anomalous state—as in the case of water at 4 °C. Here, we consider all these properties to vary as functions of temperature, as described in the next section. The computational set-up and numerical methods are detailed in [13,14]. The aspect ratio, defined as $\Gamma = D/H$, where D is the diameter, is chosen to be 1/2 to make contact with a number of experiments. The Rayleigh number (based on the conditions of the mean temperature) is fixed to be 2×10^8. The Prandtl number, also based on the conditions of the mean temperature, is 0.7.

The particular motivation for the paper is the dependence on Ra of the Nusselt number, Nu, which is the ratio of the measured heat transport to that by pure conduction for the same ΔT. This dependence has been a topic of much experimental and theoretical work, summarized most recently in [15,16]. The traditional expectation is of the form $Nu = ARa^{\beta}$ [17], perhaps with logarithmic corrections [18], but the numerical value of β is under some debate. Dimensional arguments yield a value of 1/3, whereas a somewhat more detailed analysis [18] suggests that the exponent is 1/2 at very high Ra. While recent experimental and numerical work points to the likelihood that $\beta \approx 1/3$, at least for $Ra < 10^{17}$ [19], the situation appears to be somewhat uncertain because the low-temperature helium gas data given in [20] differ from those given in [19] for $Ra > 10^{13}$. It has been proposed [21] that one possible reason for this discrepancy may be the non-Boussinesq effects. Indeed, non-Boussinesq effects are often significant in water experiments even for much lower Rayleigh numbers. Thus, a knowledge of the effect of the property gradients on heat transport is essential to understand flow physics and, particularly, to resolve the differences between the two sets of helium experiments mentioned above. With this in mind, the present paper considers the dependence of all properties with temperature, one at a time.

Governing equations and numerical set-up. – The governing equations for low Mach number conditions are given in [13,14], and are repeated here for completeness:

$$\frac{\partial \rho}{\partial t} + \nabla \cdot (\rho V) = 0, \tag{1}$$

$$\frac{\partial \rho V}{\partial t} + \nabla \cdot (\rho VV) = -\nabla p + \alpha T \hat{z} + \left(\frac{Pr}{Ra}\right)^{1/2} \nabla \cdot \left(2\mu S - \frac{2}{3}\mu(\nabla \cdot V) I\right), \tag{2}$$

$$\frac{\partial T}{\partial t} + \nabla \cdot (TV) = \left(\frac{1}{PrRa}\right)^{1/2} \frac{1}{\rho C_{\rm p}} \nabla \cdot (\lambda \nabla T). \tag{3}$$

Here, S is the symmetric part of velocity gradient tensor; V is the velocity normalized by the free-fall value U (see below), $\hat{z}$ is the unit vector in the vertical direction and I is the identity tensor; V is not divergence free. As already mentioned, the physical properties appearing in the non-Boussinesq equations are temperature dependent and non-dimensionalized by their respective values at the mean temperature, $T = T_{\rm m} = 0.5$, T being the non-dimensional temperature, equal to 1 for the bottom plate and to 0 for the top plate. The free-fall velocity, $U = \sqrt{g\alpha \Delta T H}$, is computed at $T_{\rm m}$. The sidewall is assumed to be adiabatic.

The temperature dependence of each physical property is chosen to represent a typical behaviour. We illustrate two property variations in fig. 1: one with a positive dependence on temperature and the other with a negative dependence. In both cases, the property ratio is unity at $T_{\rm m}$. These particular forms of variations are arbitrary, but apply to most fluids if the numerical coefficients are adjusted suitably. The curves shown in fig. 1 are of the form $P = b + ae^{(cT)}$, where constants a, b and c are appropriately chosen and P is scaled by the value at $T = 0.5$. Results from a linear expression will not differ qualitatively from those of the present paper. The quantity Π_P, defined as

$$\Pi_P \equiv \frac{P_{\rm h} - P_{\rm c}}{(P_{\rm h} + P_{\rm c})/2}, \tag{4}$$

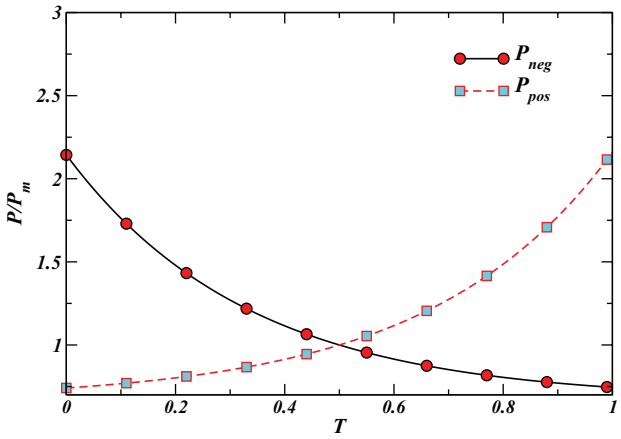

Fig. 1: Two sample functions of properties, one positively and the other negatively dependent on the temperature. These functions are arbitrary but representative of a fairly large variety of fluids. $P_{\rm m}$ corresponds to the property value at $T_{\rm m}$ and the difference between the values at $T=0$ and $T=1$ indicates the sensitivity of the property to temperature variations.

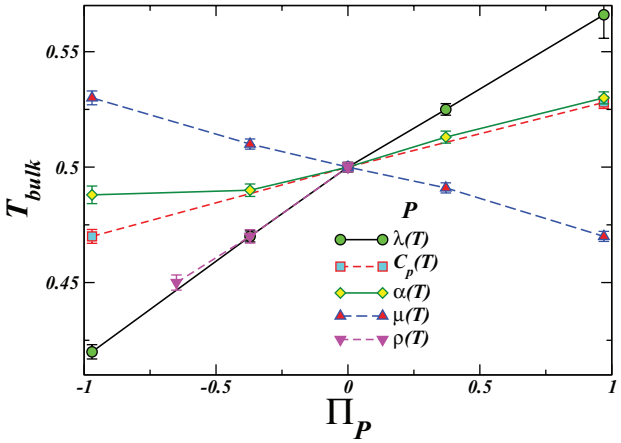

Fig. 2: Bulk temperature for different cases of Π_P. The temperature is averaged over space and time. A negative value of Π_P indicates a negative dependence on the temperature. Filled circle represents the case when only conductivity is temperature dependent, all other fluid properties being constant. Other symbols represent conditions when only one of the following properties is allowed to vary: square, $P=C_{\rm p}$; diamond, $P=\alpha$; up-triangle, $P=\mu$; down-triangle, $P=\rho$. As described in the text, Π_ρ does not extend to positive values. The error bars in this and other figures correspond to standard deviations computed from the data, as described in ref. [22].

measures the sensitivity of the property P to variations in T. Here, $P_{\rm h}$ and $P_{\rm c}$ correspond to hot and cold surfaces, respectively. A positive (negative) value of Π_P indicates a positive (negative) dependence of property P on T. The Boussinesq case corresponds to $\Pi_P=0$. Here, we calculate the Nusselt number variations against Π_P for each of the fluid properties by computing heat transport for $\Pi_P=-0.97,\ -0.37,\ 0,\ +0.37,\ +0.97$ (except for the density, see below). It may be noted that a Π_ρ (which is Π_P for density) ≈ -1 and Π_λ (which is Π_P for the thermal conductivity) ≈ 0.5 correspond to strong non-Boussinesq regimes in helium at comparable Rayleigh numbers, as discussed in [14].

The numerical grid size is $97\times49\times193$. This grid resolves the dynamics of the problem adequately, as discussed in refs. [14,22]. The heat transport is computed as the average of the heat flux at the hot and cold plates, $Nu=\overline{\lambda\partial T/\partial z}|_{\rm w}$, where $|_{\rm w}$ represents the derivative at the wall and the overbar represents the average over time and plate surface.

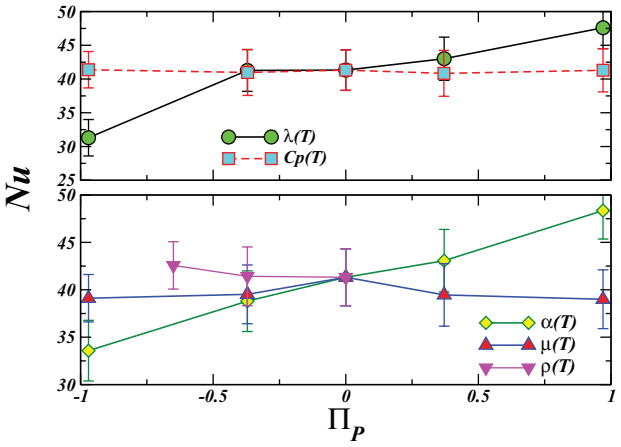

Fig. 3: The heat transport variation with respect to different values of Π_P.

Results and discussions. – We now present for all cases the bulk temperature (*i.e.*, the temperature averaged over the entire volume and time) in fig. 2, the global heat transport in figs. 3 and 4, and the buoyancy force generated at the top and bottom thermal boundary layers in fig. 5. The ratio of the top-to-bottom buoyancy flux, defined as $\langle g\alpha\Delta T_{\rm tbl}\rangle$ (the average being taken within the volume of the thermal boundary layer as well as time; the subscript denotes the thermal boundary layer), is a measure of the asymmetry created by the temperature-dependent properties. $\Delta T_{\rm tbl}$ represents the temperature difference inside the thermal boundary layer. Figure 5 shows the top-bottom ratio of the buoyancy flux ($F_{\rm B}$) against Π_P for each property P. The ratio of buoyancy flux may be written as

$$F_{\rm B}=\frac{\langle g\alpha\Delta T_{\rm tbl}\rangle_{\rm c}}{\langle g\alpha\Delta T_{\rm tbl}\rangle_{\rm h}}, \qquad (5)$$

where c and h refer to cold and hot boundary layers, respectively: the larger the deviation of this ratio from unity, the larger the asymmetry due to property gradients. If $F_{\rm B}>1$, the hot surface produces less buoyancy than the negative buoyancy produced by the cold surface.

In the following section we discuss the inferences that can be drawn from the above figures on how each of

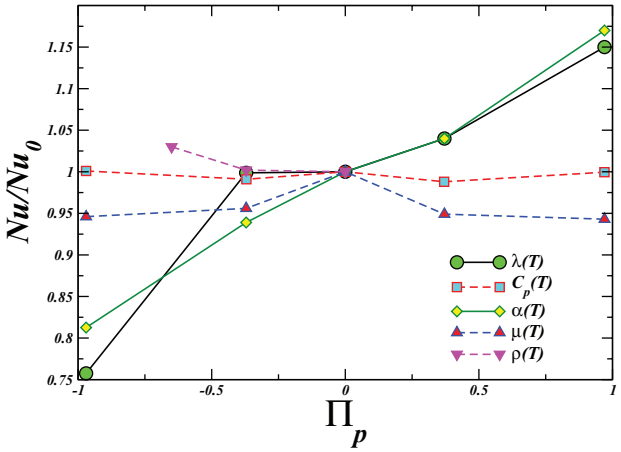

Fig. 4: The Nussel number is scaled with the value at $\Pi_P = 0$ (Nu_0 represents the Nu at $\Pi_P = 0$). The increase or decrease of heat transport is more evident in this picture.

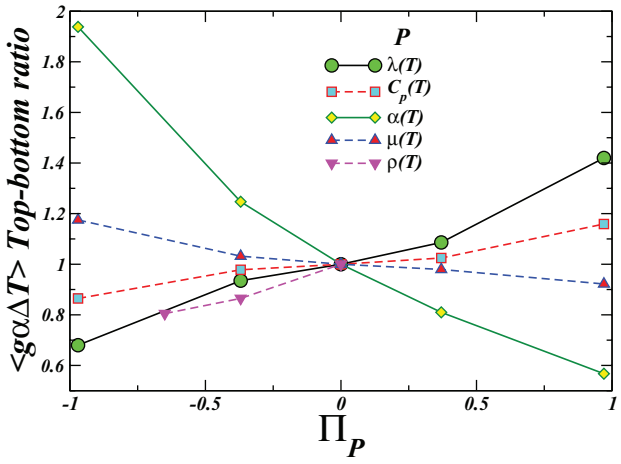

Fig. 5: The buoyancy force ratio computed within the thermal boundary layer. The buoyancy force at the top thermal boundary layer is smaller than that at the bottom if the ratio is less that unity. Deviations from unity reflect measures of asymmetry created by non-Boussinesq effect.

the properties affects the Nusselt number and the bulk temperature.

Expansivity. Both negative and positive dependences of expansivity on temperature show dramatic impact on heat transport. Figure 2 shows that the bulk temperature is lower than that for Boussinesq conditions ($\Pi_\alpha = 0$) when α is negatively dependent on temperature (a gas-like variation as described in [11]). This is easily understood looking at fig. 5 showing the top-to-bottom ratio of the fluid expansivity $g\alpha\Delta T$; in fact for negative values of Π_α, the cold fluid sinks more efficiently than the hot fluid rises, and the overall effect is to decrease the bulk temperature. The opposite behaviour is observed for $\Pi_\alpha > 0$ since buoyancy supports the uprising hot fluid more than the downcoming counterpart. It is noted that the shifts of

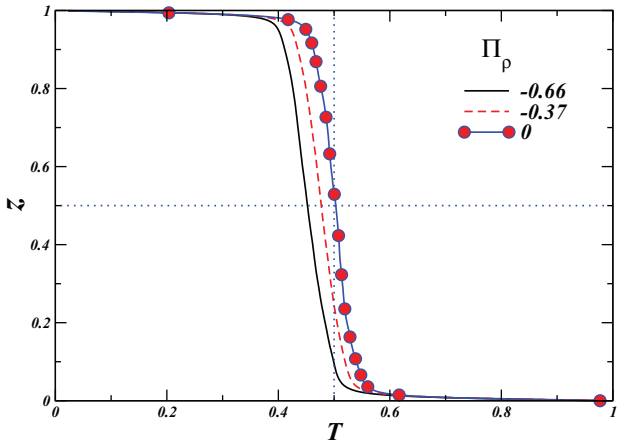

Fig. 6: Vertical temperature profile for different Π_ρ values, when density alone is varying with temperature. The driving force in Rayleigh-Bénard convection is the unstable density stratification due to ΔT. Larger negative values of Π_ρ introduce a large density difference and thus more heat transport.

the bulk temperature resemble those of ethane close to the critical point as described in [11] even if the heat transfer follows a different dynamics. In fact, while in [11] Nu increases with respect to the Boussinesq value both in the gas-like ($\Pi_\alpha < 0$) and in the liquid-like ($\Pi_\alpha > 0$) phases, for the present case Nu increases monotonically with Π_α (see figs. 3 and 4). The reason for this discrepancy is not fully understood; however, it can be argued that while in the present case only α was allowed to depend on T, in the experiments of [11] all the fluid properties varied simultaneously and the nonlinear interplay of several non-Boussinesq effects produced a different behaviour. The Rayleigh number range in [11] is also higher than that in the present study, and hence a direct comparison is not exactly possible.

Density. The density of most fluids decreases with an increase in temperature, and thus in a Rayleigh-Bènard configuration the higher-density fluid is always on the top of a lower-density fluid layer. The driving force in such a configuration is indeed the density difference. When the density depends positively on the temperature—that is, the hot fluid is heavier than the cold fluid—no convection can occur, and the heat transport is mainly due to conduction. Nevertheless, one can have transient convection for long periods of time if one starts from Boussinesq conditions (as we did). For large negative dependence on temperature, the driving force for convection is large and the Nusselt number is enhanced as shown in fig. 3. This is supported by the data in fig. 5, where the buoyancy force at the bottom is larger than that at the top, thus enhancing the convective heat transport. The heavier cold fluid moves down more readily and leads to a greater reduction in the bulk temperature, as can be seen from fig. 6. The temperature here is averaged over the radial distance r and the azimuthal angle θ, as well as over time.

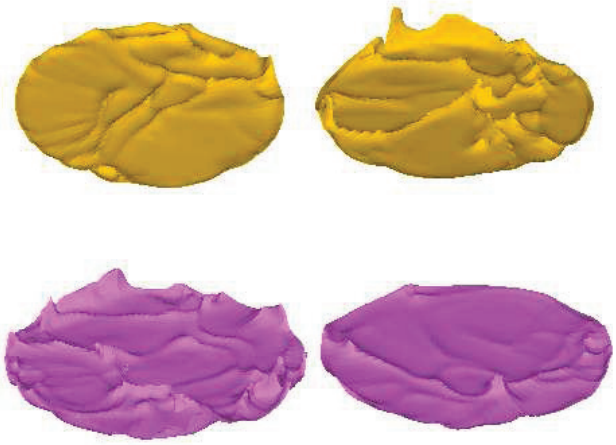

Fig. 7: Temperature isosurface for $\Pi_\mu = -0.97$ (left) and 0.97 (right). The top figures are for the isosurface corresponding to $T = 0.2$ and the bottom for $T = 0.8$. For positive values of Π_μ, the viscosity near the bottom surface is larger than that at the top surface, thus smearing the hot plume generation, as seen in the lower right figure. If Π_μ is negative, viscosity is large near the top surface, smearing the cold plumes (left top figure).

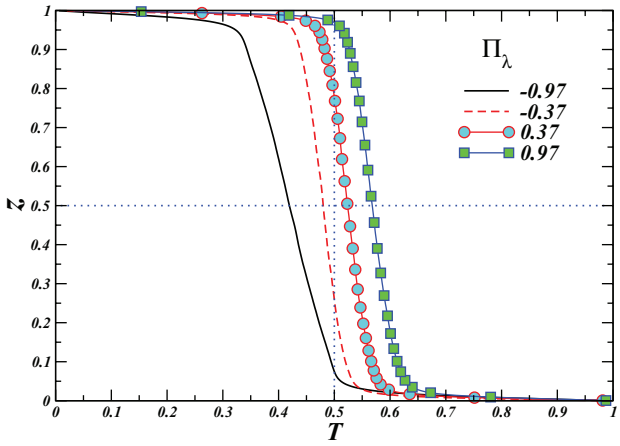

Fig. 8: Effects of temperature-dependent conductivity. Large negative Π_λ values suggest that the high-temperature region is more spread out near the hot surface, thus diminishing the heat transport from the hot surface to the bulk.

Viscosity. In [14], we reported that the role of viscosity is restricted to the smearing of plume generation, and it does not have a direct role on heat transport. The present results establish this fact further by showing the effects for negative and positive temperature variations.

The accepted mechanism of fluid motion in Rayleigh-Bénard convection is through hot plumes generated at the bottom surface and cold plumes at the top surface. A higher viscosity at the top or the bottom surface smears the respective plumes. Irrespective of whether the viscosity increases or decreases with temperature, the effect on convection is the same because the plumes are smeared at the top and bottom. However, if cold plumes are smeared, hot plumes increase the bulk temperature, as it happens for a negative temperature dependence of viscosity, and *vice versa*. Figure 2 (filled up-triangle) demonstrates this effect.

The smearing of plumes is evident from figs. 7, where the temperature isosurfaces are plotted for the top and bottom surfaces. The isosurfaces correspond to 0.2 (top row) and 0.8 (bottom row). The left and right columns represent $\Pi_\mu = -0.97$ and 0.97. For positive values of Π_μ, right column, the high viscosity near the hot surface smears the plumes that are generated, thus decreasing the bulk temperature and slightly lowering the thermal convection. Negative values of Π_μ have similar consequences near the top surface, the only difference being an increase in the bulk temperature, since cold plumes are smeared out.

Thermal conductivity. Consider first the negative temperature dependence of conductivity, with the lesser conducting fluid at the bottom. Figures 2 and 3 show that $T_{\rm bulk}$ and Nu are smaller for negative Π_λ than for the Boussinesq case. These decreases may be expected: when conductivity is small near the hot surface, there is less heat available for convection. It should be stressed that the heat transport from the hot plate to the nearby fluid is due to conduction and a lower value in conductivity means a reduction of heat transport from the plate. In short, both the Nusselt number and the bulk temperature are lower than the Boussinesq values. The fluid near the top surface, however, has larger conductivity, which will cool the fluid by conductive heat transfer. The buoyancy force at the top boundary layer may thus be expected to be smaller than that at the bottom boundary layer. Figure 5 confirms the behaviour that negative Π_λ produces smaller top-bottom buoyancy ratio. From fig. 8, we see that there is a large temperature drop at the bottom boundary layer, which also contributes to the small buoyancy ratio for negative Π_λ. It is straightforward to expect the opposite effect when conductivity increases with temperature, as is evident from figs. 2 and 3.

Specific heat. For the Rayleigh number considered here, the specific heat capacity at constant pressure, $C_{\rm p}$, does not affect the heat transport much. This negligible dependence suggests that the system can adapt to the local value of $C_{\rm p}$ in such a way that always the same amount of heat is carried by a fluid particle; however, the implication of this mechanism would be warm and cold fluid structures of different sizes over which viscosity and diffusivity would act selectively and therefore the effect of $C_{\rm p}$ cannot be separated from that of μ and λ. Concerning the bulk temperature, a small monotonic increase with $\Pi_{C_{\rm p}}$ can be observed which can be explained with the increased heat capacity (per unit volume) of the fluid that tends to carry more heat from the hot plate in the bulk.

Conclusions. – In this paper we have attempted to understand the roles of different properties in Rayleigh-Bénard convection. We analyze the heat transport and the variation of the bulk temperature due to the gradients of

these properties. The influence of each of the properties is isolated by varying only that property and holding others constant. The Rayleigh number for all the computations is fixed at 2×10^8, and so we cannot address the Rayleigh number dependence. Nevertheless, the results show that the Nusselt number is lowered by a fluid with negative dependence of the thermal conductivity, λ, and the expansion coefficient, α. A negative dependence of density introduces a larger driving force and increases the Nusselt number. Conversely, λ and α with positive dependences increase the Nusselt number. Positive temperature dependence of the density lowers the heat transport dramatically during a long transient, leading eventually to a stable state of the fluid column.

When the fluid experiences an increase in expansivity, as it happens if the latter has a large negative temperature dependence, the rising plumes block themselves and lower the bulk temperature: the heat transfer from the source (hot surface) is reduced due to reduction in convection. The negative temperature dependence of the density enhances the driving force, which means that more heat is transported; correspondingly, more cold fluid occupies larger portion of the cell, thus decreasing the bulk temperature. The role of viscosity is to smear the plume generation; cold plumes are smeared when Π_μ is negative and hot plumes are smeared when Π_μ is positive. Due to the smearing of hot and cold plumes, the fluid temperatures of the bottom and top walls are prevented from reaching the center portion of the convection apparatus, thus raising the temperature for a negative dependence and lowering it for a positive dependence. In any case, the effect of viscosity gradients is marginal.

The above results should hold qualitatively for real fluids even though the property functions described in this paper do not pertain to any particular fluid. We have not made any distinction between liquids and gases, within the assumption of low Mach number. It is a reasonable conjecture that a combination of all these effects occurs to varying degrees in a real fluid undergoing thermal convection, depending on the sensitivity of each property to the temperature.

REFERENCES

[1] Siggia E., *Annu. Rev. Fluid Mech.*, **26** (1994) 137.
[2] Kadanoff L., *Phys. Today*, **54**, issue No. 8 (2001) 34.
[3] Busse F. H., *J. Fluid Mech.*, **30** (1967) 625.
[4] Tritton D. J., *Physical Fluid Dynamics*, 2nd edition (Clarendon Press) 1988.
[5] Wu X.-Z. and Libchaber A., *Phys. Rev. A*, **43** (1991) 2833.
[6] Ahlers G. and Xu X., *Phys. Rev. Lett.*, **86** (2001) 3320.
[7] Funfschilling D., Brown E., Nikolaenko A. and Ahlers G., *J. Fluid Mech.*, **536** (2005) 145.
[8] Nikolaenko A., Brown E., Funfschilling D. and Ahlers G., *J. Fluid Mech.*, **523** (2005) 251.
[9] Ahlers G., Brown E., Araujo F. F., Funschilling D., Grossmann S. and Lohse D., *J. Fluid Mech.*, **569** (2006) 409.
[10] Ahlers G., Araujo F. F., Funschilling D., Grossmann S. and Lohse D., *Phys. Rev. Lett.*, **98** (2007) 054501.
[11] Ahlers G., Calzavarini E., Arujo F. F., Funfschilling D., Grossmann S., Lohse D. and Sugiyama K., *Phys. Rev. E*, **77** (2008) 046302.
[12] Sugiyama K., Calzavarini E., Grossmann S. and Lohse D., *EPL*, **80** (2007) 34002.
[13] Sameen A., Verzicco R. and Sreenivasan K. R., *Phys. Scr.*, **T132** (2008) 014053.
[14] Sameen A., Verzicco R. and Sreenivasan K. R., in preparation.
[15] Niemela J. J. and Sreenivasan K. R., *J. Low Temp. Phys.*, **143** (2006) 1163.
[16] Procaccia I. and Sreenivasan K. R., *Physica D*, **237** (2008) 2167.
[17] Malkus M. V. R., *Proc. R. Soc. London, Ser. A*, **225** (1954) 196.
[18] Kraichnan R. H., *Phys. Fluids*, **5** (1962) 1374.
[19] Niemela J. J., Skrbek L., Sreenivasan K. R. and Donnelly R. J., *Nature*, **404** (2000) 837.
[20] Chavanne X., Chilla F., Chabaud B., Castaing B. and Hebral B., *Phys. Fluids*, **13** (2001) 1300.
[21] Niemela J. J. and Sreenivasan K. R., *J. Fluid Mech.*, **481** (2003) 355.
[22] Verzicco R. and Camussi R., *J. Fluid Mech.*, **477** (2003) 19.